Available online at www.sciencedirect.com

ScienceDirect

Energy Procedia 148 (2018) 830–837

Energy Procedia

www.elsevier.com/locate/procedia

73rd Conference of the Italian Thermal Machines Engineering Association (ATI 2018), 12–14 September 2018, Pisa, Italy

Experimental and numerical characterization of a positive displacement vane expander with an auxiliary injection port for an ORC-based power unit

Fabio Fatigati*, Marco Di Bartolomeo, Roberto Cipollone

Università degli Studi dell'Aquila , Dipartimento di Ingegneria Industriale, dell'Informazione e di Economia, L'Aquila, Italia

Abstract

In the present work a novel technology based on a dual injection vane expander has been introduced. The component works on a power unit fed by the exhaust gases of 3L turbocharged diesel engine. The new device was tested in a wide range of operating conditions and its numerical model was validated on the experimental data. The performances of the new machine were compared to those of the original one. The results showed that the dual injection expander provided an increase of the indicated and mechanical power up to 50% and 30%. Mass flow rate can be increased by 30% and this widens the performances of the power unit; this aspect is particularly suitable for a recovery unit fed by the widely changing exhaust gases flow rates in ICEs.

Keywords: ORC; WHR; vane expander; aucxiliary injection; experimental; modelling;

* Corresponding author. Tel.:+39-0862-434623;
E-mail address: fabio.fatigati@univaq.it

Nomenclature

OEM	Original Equipment Manufacturing
P_{ind}	Indicated power [W]

10.1016/j.egypro.2018.08.114

P_{mec}	Mechanical power [W]
f	Sampling frequency [Hz]
m_{R236fa}	Working fluid mass flow rate [kg/s]
n	Revolution speed [rpm]
h_{in}	Enthalpy of working fluid at expander inlet [kJ/kg]
h_{out}	Enthalpy of working fluid at expander outlet [kJ/kg]
$h_{out, adis}$	Enthalpy of working fluid at expander outlet in adiabatic isentropic condition [kJ/kg]
$p_{exp,in}$	Pressure at expander inlet [bar_a]
$p_{exp,out}$	Pressure at expander outlet [bar_a]
η_{ind}	Indicated efficiency [%]
η_{is}	Isentropic efficiency [%]
θ_v	Vane angular extent [deg]
ω	Pulsation of the fitting function [rad/s]

1. Introduction

The always more stringent legislation on emissions and consumption reduction in ICE in the transportation sector has determined in recent years a growing interest in thermal waste recovery. In this context, the conversion of thermal energy assumes a great role considering both a direct utilization of the recovered energy and a further conversion in electric energy through electric auxiliaries. As known, the road transportation represents an important sector, responsible of a third of the final energy consumption resulting in a similar contributions to CO_2 overall emissions [1]. Even if hybrid and electric vehicles are growing in the global market it cannot be expected a mass production in the near future.

Looking into the details of the energy conversion in ICEs, an average 30% conversion efficiency from the chemical energy into mechanical power is achieved. The most important reason is the rejected heat with exhaust gases, so the recovery with mechanical energy is a challenge on which a huge literature is oriented. Among the available technologies the power units based on ORC seem to have reached a good level of development allowing the conversion through the expansion of a low boiling organic working fluid. Although there are some concerns regarding the installations of these power units on board, i.e. engine backpressure, incremental weight, radiator frontal area occupation [2], security, reliability and cost, these units demonstrate significant improvement opportunities referred in particular to the expansion machines. Depending on their operating principles expanders can be classified primarily in dynamic and positive displacement machines. Both have been extensively studied numerically and experimentally.

Turbomachines showed high isentropic efficiencies ([3],[4],[5]) varying from 0.5 to 0.8 depending on the nominal power. However there are lots of concerns regarding the high rotational speed which can determine a low mechanical to electric conversion efficiency, low flexibility of operation (especially in off-design operating conditions) [6] and vibrations. On the other hand, volumetric machines show higher flexibility with lower rotational speed. They are classified according to the geometry which realizes the expansion (scroll, screw, sliding vanes, swashing plates, piston etc.). Scroll expanders have been widely studied resulting in overall experimental efficiencies up to 80% ([7],[8]). Experimental comparisons have been made showing better results with respect to other different expander types [7]. Screw expander have a more complex geometry with slightly lower isentropic efficiencies up to 70 %, [9]. Volumetric reciprocating expanders (swashing plate and piston) have also been studied. Isentropic efficiencies for the swash plate type are in the order of 40 % while the volumetric efficiency ranges from 10 to 40 %, [10]. Piston expanders isentropic efficiencies instead are reported to range from 50 to 70 % when used with water as working fluid, [11]. Reciprocating expanders are certainly a promising technology considering the adjustable built-in volume ratio. However there are some concerns regarding size, compactness and vibrations. Sliding vane expanders have been extensively studied by the Authors ([2],[12],[13]) both numerically and experimentally showing the capability of producing up to 2 kW depending of the different upper thermal source.

To sum up, dynamic machines show greater efficiencies at the expense of high rotational speeds and much lower flexibility, which make them unsuitable to be used in applications where the hot source changes considerably. On the

other hand, volumetric expanders recover in term of operational flexibility and run at lower rotational speeds although their performances are affected by friction and volumetric losses resulting in lower overall efficiencies.

In this work, a novel technology based on the dual injection (supercharging) in a sliding-vane rotary expander has been developed. This innovation allows the increase in permeability of the machine and therefore of the whole circuit leading to a lower maximum pressure for the same working fluid mass flow rate. At the same time, at constant pressure, higher mass flow rates can be achieved with respect to the OEM expander allowing a higher recovery of the thermal energy from the exhaust gases. The second injection has been realized through an auxiliary port ([14],[15]) whose circumferential position has been optimized. The expander has been tested in a ORC unit fed by the exhaust gases of a 3L turbocharged IVECO F1C engine used both for light and heavy duty applications. Comparison have been made with the baseline expander at different operating conditions for the machine. In addition, thanks to the experimental activity a numerical model has been realized and validated to support further developments.

2. Experimental setup

The experimental study on the expander performances has been carried out on an ORC power unit shown in Figure 1 and in Figure 2. The hot source is represented by the exhaust gases of an IVECO F1C engine while the cold one by cooling water. R236fa has been used as working fluid in order to compare the experimental results with previous works, [15]. The unit consists of 4 main components: a pump, an evaporator, an expander and a condenser. The gear pump is driven by a variable speed asynchronous electric motor. The evaporator is a plate and fin heat exchanger with the exhaust gases on the fin side to prevent the increase in the exhaust pressure drop on the engine. The fluid exiting the evaporator is split in two streams feeding the two injection ports. Mass flow rate towards the auxiliary port is controlled by a valve. The mechanical energy is converted through an asynchronous electric generator with 4 magnetic poles connected to the electric network: this forces the expander to rotate at around 1500 RPM. After the expansion the working fluid is condensed by means of a plate heat exchanger and it flows inside a tank upstream the pump used to stabilize its operation. The presence of the reservoir, even though increases the plant size, produces positive effect on pump operation and minimum pressure reduction.

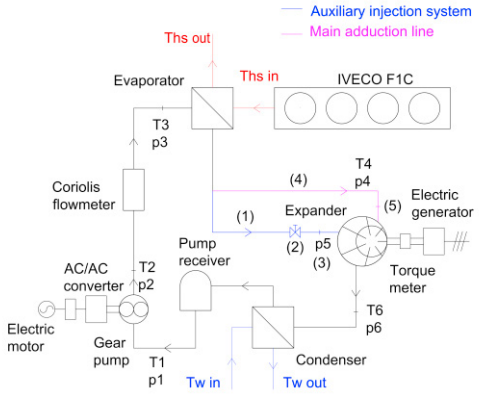

Figure 1. ORC unit scheme.

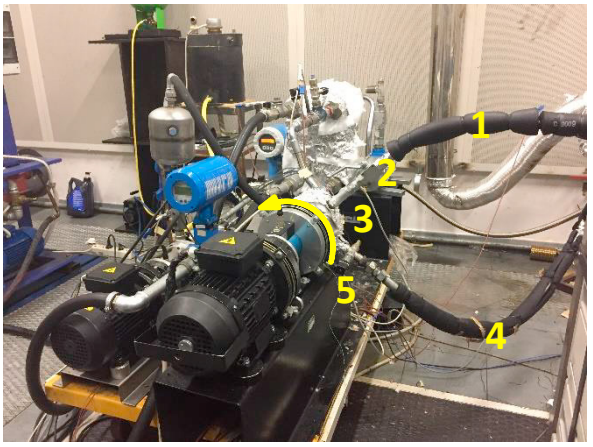

Figure 2. Experimental test bench: 1. Auxiliary suction line; 2. Regulation valve; 3 Aux. suction pressure sensor; 4 Main suction line; 5 Main suction pressure sensor.

Pressure and temperatures are measured at the points reported in Figure 1 with a sampling frequency of 4.5 kHz and 90 Hz respectively through a DAQ acquisition system. In addition 3 piezo-resistive transducers measure the pressure inside expander's vanes in three different angular positions. This way p-V cycle inside the machine has

been measured. Expander speed and torque are measured with a torque-meter mounted on the shaft. These data, together with the indicated cycle reconstructed thanks to the piezo-resistive pressure transducers allow the evaluation of the mechanical efficiency of the expander.
Piezo-resistive pressure transducers signals are post-processed to obtain the indicated cycle through an ensemble average operation. This way high frequency oscillations due to noise and squeezing phenomena are reduced. Having the procedure a certain complexity, some remarks on the used method are discussed. As it is known, the raw data of the pressure transducers require a suitable procedure to produce a p-V diagram. In order to clearly identify the angle positions pressure values are referred to, in Figure 3 a schematic of the expander is presented with the position of the sensors and the reference angles. Pressure signals from the sensors are fitted with a periodic sinusoidal function. From the frequency of this function, from the sampling frequency and from the geometry of the machine, its average rotational speed has been evaluated as in eq.1:

$$n = \frac{\theta_v}{2\pi/\omega}\frac{1}{6} \tag{1}$$

where n represents the expander speed, θ_v the vane angular width and ω the pulsation of the fitting function. When n is known, the incremental angle value Δθ can be evaluated as in eq.2:

$$\Delta\theta = n\frac{1}{6}\frac{1}{f} \tag{2}$$

where f is the sampling frequency. This way the rotational speed is evaluated with a high degree of precision not directly available from the torque meter. Only with this accuracy the p-θ diagram and then the p-V diagram can be obtained, guaranteeing an accurate reconstruction.
The position of the pressure transducers, considering the geometrical constraints, allows the evaluation of a portion of the indicated cycle equal to 154.2 degrees. For the remaining angular portion p-V data have been extrapolated from the numerical model studied and developed by the authors ([14],[15]). The uncertainty of the indicated power was evaluated according to the approach reported in [13].

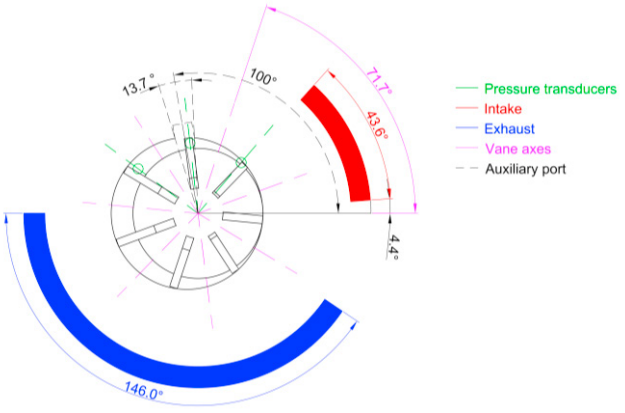

Figure 3. Details of the sliding vane expander.

Table 1. Auxiliary injection system.

Auxiliary injection system	
Auxiliary inj. line diameter	12.7 mm
Start of the aux. inj. phase	71.7 °
End of the aux. inj. phase	129.6 °
Angular extension of Aux. inj. port	13.7 °

In Table 1 the relevant data of the second injection are reported: they have been evaluated according to the same software procedure available in [14]. The auxiliary injection system has been installed on the ORC test bench and it

was composed of an auxiliary injection line (element 1 of Figure 2) that branches off from the evaporator outlet feeding the expander through the auxiliary injection port. A regulation valve (element 2 of Figure 2) allows to reduce the mass flow rate flowing inside the machine via the auxiliary injection port. The main adduction line (element 4 of Fig. 2) feeds the expander through the original suction port. Two pressure sensors measure the auxiliary and main suction pressures (element 3 and 5 of Figure 2 respectively).

3. Comparison between Baseline and Supercharged Expander

In order to assess the potential benefits of the dual injection, the expander performances were experimentally evaluated and compared with those of the OEM version. During the tests the upstream and downstream pressures were kept constant. In the case of double injection a higher mass flow rate was needed due to the higher permeability of the expander in order to keep constant the inlet pressure. The experimental data obtained reported in Table 2 allowed to assess the performances of the dual injection expander in a wide range of operating condition. Indeed, the mass flow rate varied between 0.09 and 0.14 kg/s, the Indicated Power P_{ind} between 486 and 893 W while the Mechanical Power P_{mec} between 286 and 590 W. Indicated efficiency η_{ind} was reported in eq.3 while isentropic efficiency η_{is} (eq.4) was evaluated as in [16].

$$\eta_{ind} = \frac{P_{ind}}{m_{R236fa}(h_{in} - h_{out,adis})} \tag{3}$$

$$\eta_{is} = \frac{P_{mec}}{m_{R236fa}(h_{in} - h_{out,adis})} \tag{4}$$

This definition includes the mechanical efficiency too, i.e. the ratio between the mechanical P_{mec} and the indicated P_{ind} power. Some mechanical damages appeared in the machine and this seriously limited the expander's performances. In reality, for sake of precision, in the definition the fact that the expansion is not fully adiabatic (not isentropic) but partly adiabatic and partly isochoric (at the exhaust port opening) furtherly reduces the overall efficiency as it is calculated according to eq. 4.

Table 2. Experimental characterization of the dual injection expander.

case		1	2	3	4	5	6	7	8
p_{in}	±0.3 [bar_a]	4.7	4.6	4.8	5	5.7	6	6.2	7
p_{out}	±0.3 [bar_a]	2.2	2.2	2.3	2.3	2.5	2.6	2.7	3
$p_{asp,aux}$	±0.3 [bar_a]	4.2	4.2	4.4	4.5	5.1	5.5	5.8	6.5
T_{in}	±0.3 [°C]	55	74	71	64	86	80	72	90
T_{out}	±0.3 [°C]	47	65	62	56	75	71	62	80
n	±1 [RPM]	1520	1516	1518	1518	1525	1525	1527	1536
P_{ind}	±2% [W]	501	486	523	554	700	762	813	893
P_{mec}	±0.8% [W]	286	305	320	327	450	479	494	590
$\dot{m}_{R236fa}$	±0.15%[kg/s]	0.09	0.09	0.09	0.10	0.11	0.12	0.13	0.14
η_{ind}	[%]	54.3	52.1	53.3	52.1	53.4	49.6	49.6	47.5
η_{is}	[%]	31.0	32.7	32.6	30.7	34.3	31.2	30.2	31.4

The experimental data were used to validate a numerical model of dual injection expander which was developed from the one reported in [14]. The model was developed in GT-Suite™ environment and allows to reproduce the fluid-dynamic and mechanical behavior of the expander. It represents with good accuracy the real behavior of the machine as shown in Table 3. Errors are in the range of the experimental uncertainties. Moreover, volumetric and mechanical losses can be assessed. As it can be observed from the analysis of the indicated cycle (Figure 4), after an initial decrease during the last part of the main suction phase, the pressure raises in correspondence of the auxiliary injection. When the auxiliary suction phase is ended, the pressure sharply decreases.

Table 3. Absolute relative percentage error between experimental and numerical data.

case		1	2	3	4	5	6	7	8
e_{Pind}	[%]	2.0%	1.8%	1.1%	0.0%	-3.6%	-4.3%	-3.7%	-5.2%
e_{Pmech}	[%]	-0.7%	-0.6%	-0.6%	-0.6%	-0.5%	-0.6%	-0.6%	-0.6%
e_{m236fa}	[%]	-0.2%	2.6%	1.9%	0.5%	-2.5%	2.2%	0.5%	-0.4%

Generally, the pressure inside the vane at the start of the discharge phase is larger than the pressure at the condenser thus a quite strong isochoric expansion takes place (Figure 4-Figure 5). The two vertical dashed lines reported in Figure 4 and Figure 5 represent the volume of the vane when the auxiliary injection starts ("Start aux. inj. Volume) and when the auxiliary injection ends (End aux. inj. Volume). As it can be observed from the Figure 4, the model allows to reproduce with good accuracy the experimental trend. In particular, an interesting feature for further improvements is the non-isobaric filling of the machine the experimental and numerical p-V diagrams show. This is due to the volumetric losses and to the volume increase during suction phase. Moreover, the numerical model was able to reproduce the increasing of pressure during the auxiliary injection phase and the fluid expansion.

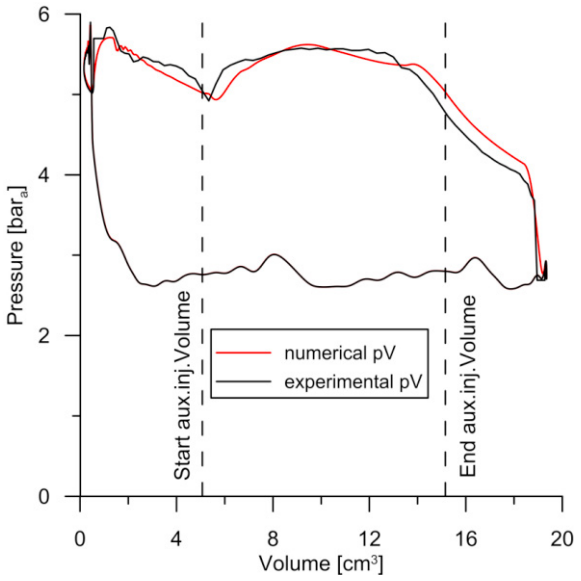

Figure 4: Comparison between experimental and numerical indicated cycle for the case 7 of Table 3.

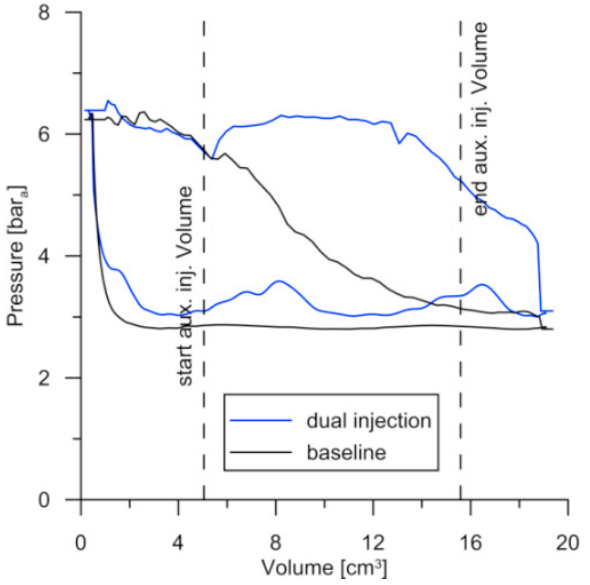

Figure 5: Experimental comparison between dual injection and baseline expanders keeping constant the main suction pressure.

In Figure 5 and Table 4 the results of the experimental comparison between the two devices has been reported. They show that the indicated and mechanical power increases respectively by 62% and 37% adopting the dual injection. Indeed, the injection of working fluid through the auxiliary suction port delays the pressure decrease due to the expansion as happens in OEM device. As it can be observed from the experimental results reported in Table 5 the dual injection expander allows a greater mass flow rate of working fluid than the OEM device (up to 30%), resulting from keeping the same upstream pressure. Indeed, the dual injection increases the permeability of the machine. It would be expected that if the mass flow rate is constant the suction pressure of the OEM is higher than the dual injection expander. Indeed, as reported in Figure 6, the dual injection expander is seen by the circuit as a lower pressure drop Δp for a same value of mass flow rate of working fluid. The introduction of auxiliary injection causes an increase of the indicated efficiency η_{ind} (eq.3) due to the higher pressures during the vane expansion. This appears certainly a positive aspect. Concerning the isentropic efficiency a wider testing activity is still needed considering the appearance of some damages which occurred during testing. These damages increased the mechanical power lost

due to friction (Table 2,4,5), seriously limiting the conversion into useful power (shaft power) which was expected and which was confirmed by the first tests done.

Table 4: Experimental comparison between Dual injection and OEM expanders performance keeping constant the main suction pressure.

	$p_{exp,in}$ ± 0.3 [bar_a]	$p_{exp,out}$ ±0.3 [bar_a]	$\dot{m}_{R236fa}$ ± 0.15% [kg/s]	P_{ind} ± 2% [W]	P_{mec} ± 2% [W]	η_{ind} [%]	η_{ind} [%]
Dual inj. exp.	6.3	3.1	0.14	843	590	34	48
OEM expander	6.2	2.8	0.10	521	432	32	39

Tab. 5. Experimental comparison between dual injection and baseline expander.

case		9	10	11	12	13	14	15
Dual. Inj. Exp.	$p_{exp,in}$	6.6	5.6	6.4	6.4	6.6	6.3	4.5
Baseline Exp.	± 0.3 [bar_a]	6.7	5.6	6.4	6.4	6.7	6.3	4.6
Dual. Inj. Exp.	$p_{exp,out}$	3.3	2.8	3.1	3.1	3.1	3.0	2.4
Baseline Exp.	±0.3 [bar_a]	3.1	2.8	3.0	3.1	3.1	3.1	2.3
Dual. Inj. Exp.	P_{ind}	921	758	929	909	940	911	587
Baseline Exp.	± 2% [W]	585	445	577	666	651	776	504
Dual. Inj. Exp.	P_{mec}	572	462	608	606	621	595	341
Baseline Exp.	± 2% [W]	469	356	446	575	498	508	332
Dual. Inj. Exp.	$\dot{m}_{R236fa}$	0.15	0.13	0.14	0.14	0.14	0.14	0.11
Baseline Exp.	± 0.15% [kg/s]	0.11	0.08	0.11	0.12	0.10	0.13	0.09
Dual. Inj. Exp.	η_{ind}	50.9	50.4	49.2	48.2	47.3	49.2	52.1
Baseline Exp.	[%]	44.0	46.7	45.0	47.0	47.6	50.7	50.9
Dual. Inj. Exp.	η_{is}	31.6	30.7	32.2	32.1	31.2	32.2	30.3
Baseline Exp.	[%]	35.3	37.4	34.7	40.5	36.4	33.2	33.5

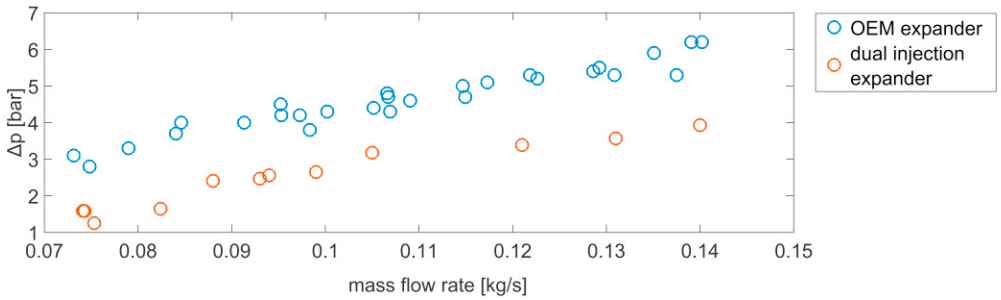

Figure 6: Difference between upstream and downstream pressure Δp [bar] as a function of the working fluid mass flow rate [kg/s].

4. Conclusions

In this paper the results of an experimental and numerical characterization of a dual injection vane expander have been reported. An ORC Power unit, whose high thermal source is represented by the exhaust gases of an IVECO F1C ICE, was developed and fully instrumented. The performances of the supercharged expander have been compared with those of the OEM with the following results:

- The dual injection expander provides an average indicated power up to 50% higher than that produced by the baseline expander. On the other hand, the mechanical power (shaft power) increased only by 30% (with respect to the OEM device) because of the increase of the power lost by friction due to the appearance of some mechanical damages of the machine;
- The dual injection expander shows an average increase of mass flow rate of about 35-40% with respect to the OEM: this gives a greater flexibility in terms of thermal power recovered.

It was demonstrated that the dual injection expander is a more permeable device than the OEM one for a fixed pressure difference between suction and exhaust section. Hence, for a fixed working fluid mass flow rate, the upstream pressure of the expander decreases, pushing the thermodynamic cycle to lower maximum pressures; for a fixed upstream pressure, a greater flow rate is achieved, thus improving the energy recovery.

Aknowledgement

The authors acknowledge Ing. Enea Mattei S.p.A and in particular its CEO, Dr. Giulio Contaldi, and Dr. Stefano Murgia Research Manager for the support during the experimental set up of the machine. The authors are grateful to Abruzzo Region for having funded this research work in the framework of PAS FSC project “STEVE”.

References

[1]. European Union. (2017). Statistical Pocketbook 2017: EU transport. Publications Office of the European Union. https://doi.org/10.2832/47741

[2]. Di Battista, D., Di Bartolomeo, M., Villante, C., & Cipollone, R. (2018). On the limiting factors of the waste heat recovery via ORC-based power units for on-the-road transportation sector. Energy Conversion and Management, 155(July 2017), 68–77. https://doi.org/10.1016/j.enconman.2017.10.091

[3]. Alshammari, F., Pesyridis, A., Karvountzis-Kontakiotis, A., Franchetti, B., & Pesmazoglou, Y. (2018). Experimental study of a small scale organic Rankine cycle waste heat recovery system for a heavy duty diesel engine with focus on the radial inflow turbine expander performance. Applied Energy, 215(October 2017), 543–555. https://doi.org/10.1016/j.apenergy.2018.01.049

[4]. Guillaume, L., Legros, A., Desideri, A., & Lemort, V. (2017). Performance of a radial-inflow turbine integrated in an ORC system and designed for a WHR on truck application: An experimental comparison between R245fa and R1233zd. Applied Energy, 186, 408–422. https://doi.org/10.1016/j.apenergy.2016.03.012

[5]. Kang, S. H. (2012). Design and experimental study of ORC (organic Rankine cycle) and radial turbine using R245fa working fluid. Energy, 41(1), 514–524. https://doi.org/10.1016/j.energy.2012.02.035

[6]. Cipollone, R., Di Battista, D., & Bettoja, F. (2017). Performances of an ORC power unit for Waste Heat Recovery on Heavy Duty Engine. Energy Procedia, 129, 770–777. https://doi.org/10.1016/j.egypro.2017.09.132

[7]. Dumont, O., Dickes, R., & Lemort, V. (2017). Experimental investigation of four volumetric expanders. Energy Procedia, 129, 859–866. https://doi.org/10.1016/j.egypro.2017.09.206

[8]. Lemort, V., Quoilin, S., Cuevas, C., & Lebrun, J. (2009). Testing and modeling a scroll expander integrated into an Organic Rankine Cycle. Applied Thermal Engineering, 29(14–15), 3094–3102. https://doi.org/10.1016/j.applthermaleng.2009.04.013

[9]. Pantano, F., & Capata, R. (2017). Expander selection for an on board ORC energy recovery system. Energy, 141, 1084–1096. https://doi.org/10.1016/j.energy.2017.09.142

[10]. Galindo, J., Ruiz, S., Dolz, V., Royo-Pascual, L., Haller, R., Nicolas, B., & Glavatskaya, Y. (2015). Experimental and thermodynamic analysis of a bottoming Organic Rankine Cycle (ORC) of gasoline engine using swash-plate expander. Energy Conversion and Management, 103, 519–532. https://doi.org/10.1016/j.enconman.2015.06.085

[11]. Glavatskaya, Y., Podevin, P., Lemort, V., Shonda, O., & Descombes, G. (2012). Reciprocating expander for an exhaust heat recovery rankine cycle for a passenger car application. Energies, 5(6), 1751–1765. https://doi.org/10.3390/en5061751

[12]. Cipollone, R., Bianchi, G., Di Battista, D., Contaldi, G., & Murgia, S. (2014). Mechanical energy recovery from low grade thermal energy sources. Energy Procedia, 45(February), 121–130. https://doi.org/10.1016/j.egypro.2014.01.014

[13]. Giuseppe Bianchi, Roberto Cipollone, Theoretical modeling and experimental investigations for the improvement of the mechanical efficiency in sliding vane rotary compressors, Applied Energy, Volume 142, 2015, Pages 95-107, ISSN 0306-2619, https://doi.org/10.1016/j.apenergy.2014.12.055.

[14]. Fabio Fatigati, Giuseppe Bianchi, Roberto Cipollone, Development and numerical modelling of a supercharging technique for positive displacement expanders, Applied Thermal Engineering,2018,ISSN 1359-4311, https://doi.org/10.1016/j.applthermaleng.2018.05.046.

[15]. Fabio Fatigati (2017). Exhaust gases waste heat recovery in ICEs: theoretical and experimental characterization of innovative technologies and plant solutions. PhD thesis.

[16]. Vaclav Vodicka, Vaclav Novotny, Jakub Mascuch, Michal Kolovratnik,Impact of major leakages on characteristics of a rotary vane expander for ORC, Energy Procedia,Volume 129,2017,Pages 387-394,ISSN 1876-6102,https://doi.org/10.1016/j.egypro.2017.09.249.